Cell Metabolism
Article

TORC2 Regulates Hepatic Insulin Signaling via a Mammalian Phosphatidic Acid Phosphatase, LIPIN1

Dongryeol Ryu,[1,6] Kyoung-Jin Oh,[1,6] Hee-Yeon Jo,[1] Susan Hedrick,[2] Yo-Na Kim,[3] Yu-Jin Hwang,[3] Tae-Sik Park,[3] Joong-Soo Han,[5] Cheol Soo Choi,[3,4] Marc Montminy,[2] and Seung-Hoi Koo[1,*]
[1]Department of Molecular Cell Biology, Sungkyunkwan University School of Medicine, 300 Chunchun-dong, Jangan-gu, Suwon, Gyeonggi-do 440-746, Korea
[2]Peptide Biology Laboratories, Salk Institute for Biological Studies, La Jolla, CA 92037, USA
[3]Lee Gil Ya Cancer and Diabetes Institute
[4]Division of Endocrinology
Gil Medical Center, Gachon University of Medicine and Science, Incheon 405-760, Korea
[5]Institute of Biomedical Science and Department of Biochemistry and Molecular Biology, College of Medicine, Hanyang University, Seoul 133-791, Korea
[6]These authors contributed equally to this work
*Correspondence: shkoo@med.skku.ac.kr
DOI 10.1016/j.cmet.2009.01.007

SUMMARY

TORC2 is a major transcriptional coactivator for hepatic glucose production. Insulin impedes gluconeogenesis by inhibiting TORC2 via SIK2-dependent phosphorylation at Ser171. Interruption of this process greatly perturbs hepatic glucose metabolism, thus promoting hyperglycemia in rodents. Here, we show that hyperactivation of TORC2 would exacerbate insulin resistance by enhancing expression of LIPIN1, a mammalian phosphatidic acid phosphatase for diacylglycerol (DAG) synthesis. Diet-induced or genetic obesity increases *LIPIN1* expression in mouse liver, and TORC2 is responsible for its transcriptional activation. While overexpression of LIPIN1 disturbs hepatic insulin signaling, knockdown of LIPIN1 ameliorates hyperglycemia and insulin resistance by reducing DAG and PKCε activity in *db/db* mice. Finally, TORC2-mediated insulin resistance is partially rescued by concomitant knockdown of LIPIN1, confirming the critical role of LIPIN1 in the perturbation of hepatic insulin signaling. These data propose that dysregulation of TORC2 would further exaggerate insulin resistance and promote type 2 diabetes in a LIPIN1-dependent manner.

INTRODUCTION

Insulin resistance is a major predicament for the development of type 2 diabetes. Increased infusion of free fatty acids into the peripheral tissues due to the atherogenic diets or obesity directs to the accumulation of intracellular free fatty acids, which then leads to the generation of various second messengers for signaling cascades, including diacylglycerol (DAG), a major activator for protein kinase C (PKC) families (Savage et al., 2007). Among family members, PKCε is known to be involved in reducing insulin receptor (IR) kinase activity, thus inhibiting insulin-mediated signaling cascades in liver (Samuel et al., 2004, 2007).

Previously identified as a gene product that is responsible for the pathophysiology of *fld* mice, which show occurrence of neonatal fatty liver that is accompanied by hypertriglyceridemia and lipodystrophy phenotypes, LIPIN1 is later shown to be involved in various pathways in lipid metabolism in diverse cell types such as liver, adipose tissues, muscle, and neuronal cells (Finck et al., 2006; Peterfy et al., 2001, 2005; Phan et al., 2004; Phan and Reue, 2005; Reue and Zhang, 2008; Verheijen et al., 2003). Depletion of *LIPIN1* gene in preadipocytes delays the fat cell differentiation, and *fld* mice that lack expression of functional LIPIN1 display lipodystrophy-associated insulin resistance, perhaps due to the lack of adipokine generation, showing the importance of adipose-specific LIPIN1 function in lipid homeostasis and systemic insulin signaling. On the other hand, muscle-specific *LIPIN1* transgenic mice show insulin resistance and obesity phenotypes, suggesting the presence of differential functions of LIPIN1 in different cell types. The role of LIPIN1 in liver is somewhat more complicated. LIPIN1 appears to function as a coactivator for PPARα/PGC-1α to transcriptionally regulate fatty acid oxidation gene expression. At the same time, two recent reports suggest contradicting results regarding functions of LIPIN1 in the regulation of triglyceride synthesis and VLDL secretion, depending on the systems utilized (Chen et al., 2008; Khalil, 2009). The presence of other isoforms, LIPIN2 and LIPIN3, makes it hard to determine the sole contribution of LIPIN1 in hepatic lipid metabolism (Reue and Dwyer, 2008). Surprisingly, LIPIN1 is later identified as a cytosolic phosphatidic acid phosphatase (PAP) that would generate DAG in response to increase in intracellular free fatty acid levels (Carman and Han, 2006; Donkor et al., 2007; Han et al., 2006, 2007; Reue and Zhang, 2008). The PAP function of LIPIN1 could potentially link this protein with free fatty acid-induced perturbation of insulin signaling that is observed in muscle-specific *LIPIN1* transgenic mice (Phan and Reue, 2005).

TORC2 is a major transcriptional coregulator for hepatic glucose output in response to fasting in mammals (Koo et al., 2005). While fasting triggers a rapid dephosphorylation and nuclear entry of TORC2 to promote hepatic gluconeogenesis,

feeding induces insulin signaling cascades that would enhance the activity of inhibitory serine/threonine kinase SIK2 to reverse the process by phosphorylating Ser171 residue of TORC2, resulting in the retention of this factor in the cytoplasm in association with 14-3-3 proteins (Dentin et al., 2007; Screaton et al., 2004). During insulin-resistant conditions, however, TORC2 remains in the nucleus and is actively involved in coactivating CREB-target gluconeogenic gene expression, in part due to the inactivation of AKT-mediated SIK2, which results in hyperglycemia that would further exacerbate the insulin-resistant phenotype and ultimately bring about the type 2 diabetes.

Here, we report that TORC2 transcriptionally activates *LIPIN1* expression during fasting and insulin-resistant conditions in mouse liver. Overexpression of LIPIN1 in primary hepatocytes indeed increases DAG production and results in inactivation of AKT due to the activation of PKCε. Furthermore, adenovirus-mediated knockdown of hepatic LIPIN1 in diabetic *db/db* mice greatly alleviates hyperglycemia as well as hepatic insulin resistance. These data support that TORC2-mediated induction of *LIPIN1* expression during insulin resistance would greatly contribute to the further exacerbation of hyperglycemia and the progression of type 2 diabetes.

RESULTS

S171A TORC2 Promotes Hepatic Insulin Resistance

As reported previously, Ser171 residue of TORC2 is targeted by AMPK and AMPK-related kinases, including SIK kinases, and is critical for determining its cellular localization (Koo et al., 2005; Shaw et al., 2005). Mutation of this residue into alanine results in constant nuclear localization of TORC2, which leads to the unregulated activation of TORC2/CREB target genes. Indeed, mice injected with adenovirus for Ser171 to alanine mutant TORC2 (S171A TORC2) show higher blood glucose levels as well as increased expression of gluconeogenic genes (Figures 1A and 1C) relative to mice with GFP control adenovirus injection. Unexpectedly, S171A TORC2 mice show impaired glucose tolerance compared with GFP mice (Figure 1B). We would speculate this is due to either the increased gluconeogenic/decreased glycolytic gene expression or the increased TORC2 target gene expression in S171A mouse that would potentially perturb insulin signaling in this setting.

LIPIN1 Is a Transcriptional Target of TORC2 in Liver

To gain a further insight into the nature of this phenomenon, we performed microarray analysis using RNAs from mouse liver infected with either TORC2 RNAi adenovirus or US control RNAi adenovirus. As shown previously, several TORC2/CREB target genes in the gluconeogenesis are downregulated by TORC2 knockdown in microarray analysis (Table 1) and are confirmed by quantitative PCR (Q-PCR) (Figure 1E). Knockdown of TORC2 does not promote changes in expression of several glycolytic enzyme genes. Surprisingly, we noticed a change in gene expression levels of *LIPIN1*, a member of mammalian PAP families, by TORC2 knockdown. Fasting and either diet-induced or genetic insulin resistance in mouse enhance hepatic *LIPIN1* expression (Figures 2A, 2B, and S1–S4), while SIK expression greatly inhibits it (Figures S5–S7), showing similar regulatory patterns with gluconeogenic *PEPCK* gene in these settings. Indeed, we were able to confirm the increased expression of *LIPIN1*, but not of *LIPIN2* or *3*, by S171A TORC2 infection in mouse liver or in primary hepatocytes (Figures 1C, 1D, and 2C). Furthermore, expression of *LIPIN1* is increased by TORC2 and inhibited by CREB inhibitor ACREB in primary hepatocytes, further confirming that TORC2/CREB might regulate *LIPIN1* expression in liver (data not shown). To verify whether TORC2/CREB would regulate *LIPIN1* expression at the transcriptional level, we obtained *LIPIN1* promoter from mouse genomic DNA and performed transient transfection assays in HepG2 cells. We chose to utilize sequences upstream of exon 1b as a hepatic promoter for *LIPIN1*, since exon 1b appears to be selectively expressed over exon 1a in hepatocytes. Moreover, hepatic *LIPIN1* transcript with exon 1b is regulated by fasting or insulin–resistance mouse models, as shown by RT-PCR analysis using differential exon-specific primers (Figure S8). Interestingly, *LIPIN1* promoter is upregulated by TORC2 cotransfection in the presence of PKA, and TORC2-/cAMP-responsive region is localized −85 to +56 from the putative transcriptional start site (Figures 2D and 2E). TORC2 occupies promoter regions of several CREB target genes, such as *PEPCK* or *G6Pase*, and the occupancy of TORC2 on the *LIPIN1* promoter is also confirmed by chromatin immunoprecipitation assay in mouse primary hepatocytes, further confirming that TORC2 regulates *LIPIN1* expression at the transcriptional level in vivo (Figure 2F).

LIPIN1 Expression Increases DAG Production and Inhibits Insulin Signaling in Primary Hepatocytes

Increased production of DAG is linked to obesity-related insulin resistance in peripheral tissues (Samuel et al., 2004, 2007; Savage et al., 2007). Since LIPIN1 was previously reported as a mammalian cytosolic PAP in other cell types, we wanted to verify whether this protein functions similarly in liver. Adenovirus-mediated overexpression of wild-type (WT) LIPIN1 or LIPIN2 induces DAG production in response to palmitate treatment, while LIPIN1 with mutations in previously defined phosphatase active sites does not promote such events in primary hepatocytes (Figures 3A and S9). In accordance with increased DAG production by WT LIPIN1, Ser729 phosphorylation of PKCε, a major noncanonical PKC isoform in liver, is much more pronounced with WT LIPIN1-infected cells compared with cells infected with GFP or PAP mutant LIPIN1 in response to phosphatidic acid (PA) treatments, a direct substrate for LIPIN1 (Figure 3C). In addition, Ser473 phosphorylation of AKT is accordingly more dramatically reduced in WT LIPIN1 infected cells with treatment of PA (over 34-fold in WT LIPIN1 versus less than 10-fold in PAP mutant LIPIN1) (Figures 3B and 3C), suggesting that increased expression of LIPIN1 in the abundance of its substrates could promote insulin resistance in liver. To test whether the disturbance of insulin signaling may affect gluconeogenic gene expression, we infected primary hepatocytes with GFP control, WT LIPIN1, or PAP mutant LIPIN1 adenoviruses in the absence or in the presence of PA/insulin. Expression of either WT or PAP mutant LIPIN1 does not promote significant changes in *PGC-1α* or *PEPCK* mRNA levels in the absence or in the presence of PA without insulin treatment (Figure 3D). As expected, short-term treatment of insulin (4 hr) dramatically reduces mRNA levels of both genes. Indeed, PA treatment slightly blocks insulin-mediated inhibition of *PEPCK* gene

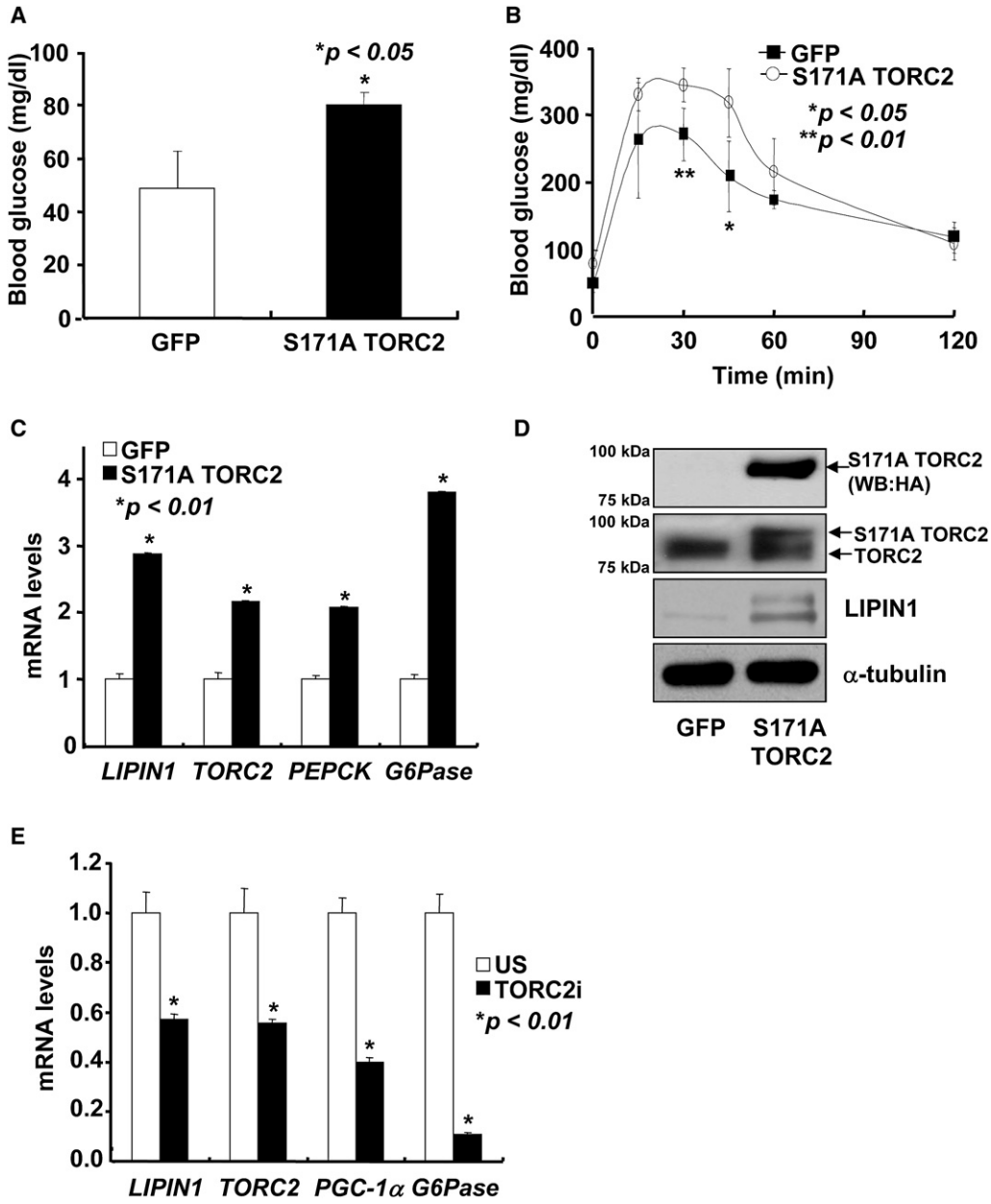

Figure 1. TORC2 Promotes Elevations in Blood Glucose Levels and Glucose Intolerance

(A) Sixteen hour fasting glucose levels in mice expressing Ad-GFP or Ad-S171A TORC2 (*p < 0.05; n = 3).

(B) Glucose tolerance test (GTT) of Ad-GFP and Ad-S171A TORC2 mice (*p < 0.05; **p < 0.01; n = 3).

(C) Effects of Ad-S171A TORC2 infection on *LIPIN1* gene expression; Q-PCR analysis of hepatic *LIPIN1*, *TORC2*, *PEPCK*, and *G6Pase* expression using hepatic RNAs from Ad-GFP or Ad-S171A TORC2-injected mice (*p < 0.01; n = 3).

(D) Western blot analysis of hepatic TORC2 and LIPIN1 levels in mice infected with Ad-GFP or Ad-S171A TORC2 virus. HA-TORC2 levels are shown on the top panel.

(E) Effects of TORC2 knockdown on *LIPIN1* gene expression; Q-PCR analysis of hepatic *LIPIN1*, *TORC2*, *PEPCK*, and *G6Pase* expression using hepatic RNAs from Ad-US control RNAi adenovirus or Ad-TORC2 RNAi virus-injected mice (*p < 0.01; n = 3). Data in (A)–(C) and (E) represent mean ± SD.

expression; the effect of PA is significantly augmented by overexpression of WT but not PAP mutant LIPIN1. These data suggest that LIPIN1 may not directly regulate gluconeogenic expression at the transcriptional level, but block insulin-dependent regulation of these genes by disturbing hepatic insulin signaling via its DAG-producing activity.

Knockdown of Hepatic LIPIN1 Improves Diabetic Conditions in *db/db* Mice

To verify the functional significance of LIPIN1 in the insulin resistance in vivo, we prepared adenovirus for *LIPIN1* shRNA and injected it into the *db/db* diabetic mice, widely utilized rodent models displaying peripheral insulin resistance. Interestingly,

Table 1. Results of cDNA Microarray Data

	Gene symbol	Fold induction
shTORC2/US	*LIPIN1**	0.733
	LIPIN2	1.018
	LIPIN3	1.131
	*G6pase**	0.478
	*PGC-1α**	0.809
	PC	0.803
	FBP1	0.702
	GCK	1.023
	PFK1	0.871
	ADOLB	1.192
	PFKFB2	0.923

G6pase, glucose-6-phosphatase; *PGC-1α*, peroxisome proliferator-activated receptor gamma coactivator 1 α; *PC*, pyruvate carboxylase; *FBP1*, Fructose-1,6-bisphosphatase 1;. *GCK*, glucokinase; *PFK1*, liver-type phosphofructokinase; *ALDOB*, aldolase B; *PFKFB2*, 6-phosphofructo-2-kinase/fructose-2,6-bisphosphatase 2. n = 3, C57BL/6, liver.
*Confirmed by Q-PCR (Figure 1E).

LIPIN1 expression is highly induced in livers of diabetic mice, as shown in Figure 2B and in the previous report (Finck et al., 2006). Knockdown of hepatic LIPIN1 is verified by Q-PCR as well as western blot analysis (Figures 4C, 4D, and 5A). Surprisingly, LIPIN1 knockdown greatly lowers blood glucose level that is associated with reduction in key gluconeogenic gene expression (Figures 4A, 5A, and S10). Moreover, intraperitoneal glucose tolerance test (GTT) reveals the improvement in glucose intolerance of *db/db* mice with LIPIN1 knockdown compared with mice with control viruses, suggesting a notion of increased hepatic insulin sensitivity with reduced hepatic LIPIN1 expression (Figure 4B). Indeed, tyrosine phosphorylation of IR, as well as serine phosphorylation of AKT, FOXO1, and GSK3β, is greatly increased by LIPIN1 knockdown both in basal and insulin-induced conditions (Figures 4C, 4D, and S11). While there are no changes in plasma TAG and NEFA levels (Figure S12), hepatic DAG and TAG levels are greatly reduced with Ad-LIPIN1 RNAi infection (Figure 5B). Moreover, phosphorylation level of PKCε is also significantly diminished (Figures 4C and 4D), further corroborating the notion that hepatic LIPIN1 knockdown improves insulin sensitivity in insulin-resistant conditions. To further evaluate the functional consequences of LIPIN1 deficiency in insulin and glucose metabolism in vivo, we performed the 140 min hyperinsulinemic-euglycemic clamp studies in conscious *db/db* mice. Basal hepatic glucose production of LIPIN1 knockdown mice tends to be lower than that of control mice ($p = 0.09$) (Figure 5C). During the clamp periods, plasma insulin was infused at a constant rate (30 pmol/kg/min) to raise plasma insulin within a physiological range, and plasma glucose was clamped at about 6.7 mM. Indeed, knockdown of LIPIN1 increases hepatic insulin sensitivity, as reflected by ~70% higher suppression of endogenous glucose production from LIPIN1-deficient mice compared to control groups (Figure 5C). However, there are no significant differences in whole-body glucose uptake, glycolysis, and glycogen synthesis between the two groups (Figure 5E). Consistent with no changes in peripheral insulin sensitivity other than that of liver, muscle glucose uptake does not show differences between the two groups of mice (Figure 5D).

LIPIN1 Knockdown Prevents S171A TORC2-Induced Insulin Resistance

Finally, we wanted to confirm whether S171A TORC2-induced glucose intolerance in mice is due to the increased expression of *LIPIN1*. Thus, Ad-LIPIN1 RNAi virus was coinjected with Ad-S171A TORC2 virus in normal mice and compared with Ad-GFP + Ad-US groups and Ad-S171A TORC2 + Ad-US groups. Ad-GFP + Ad-LIPIN1 RNAi group is not included, since we did not observe changes in blood glucose or glucose tolerance with LIPIN1 knockdown only in WT mice (data not shown). Indeed, the elevation of both 4 hr fasting and regular-feeding blood glucose levels caused by S171A TORC2 expression alone is resolved by the additional infection of LIPIN1 RNAi adenovirus (Figures 6A and 6B). Consistent with the role of LIPIN1 in the disturbance of insulin-mediated regulation of gluconeogenic gene expression, LIPIN1 RNAi-mediated reduction of *PEPCK*, *G6Pase*, or *PGC-1α* mRNA levels is much more pronounced in feeding conditions than in 4 hr fasting conditions (Figure 6E). Improved insulin sensitivity is also indicated by enhanced glucose clearance in GTT assay with S171A TORC2 + LIPIN1 RNAi groups over S171A TORC2 + US mice (Figure 6C). Moreover, reduction in serine phosphorylation of AKT or FOXO1 and induction of serine phosphorylation of PKCε in S171A TORC2 mice are restored to control levels by additional LIPIN1 knockdown both in basal state and insulin-injected conditions, showing that S171A TORC2-mediated insulin resistance is indeed partially rescued by LIPIN1 deficiency (Figures 6D and S13). The insulin levels tend to be lower with S171A TORC2 + LIPIN1 RNAi groups over S171A TORC2 + US mice under both 4 hr fasting and feeding conditions, reflecting the normalized glycemia in this setting (Figure S14).

DISCUSSION

TORC2 has been shown to be a major regulator for hepatic glucose production by directing transcriptional activation of gluconeogenic genes (Koo et al., 2005). In our study, we would now suggest another role for this coactivator as an instigator of the hepatic insulin resistance by activating LIPIN1. Hepatic expression of LIPIN1, a member of mammalian Mg^{2+}-dependent PAPs, is transcriptionally controlled by TORC2 in a CREB-dependent manner. Hepatic *LIPIN1* expression is higher in mouse models with diet-induced or genetic obesity and insulin resistance, conditions previously associated with constitutive activation of TORC2 due to the impaired insulin actions (Dentin et al., 2007; Screaton et al., 2004). We found that high-level expression of LIPIN1 increases intracellular DAG levels and perturbs insulin signaling in part via a PKCε-mediated pathway. We showed that reducing LIPIN1 expression in liver indeed improves hepatic insulin sensitivity and normalizes hyperglycemia by reducing hepatic DAG levels and PKCε activity in diabetic *db/db* mice. Furthermore, constitutively active TORC2-mediated hepatic insulin resistance is partially blunted by concomitant knockdown of LIPIN1, suggesting that TORC2-dependent expression of LIPIN1 could indeed be responsible for this phenomenon (see Figure 6F for a model).

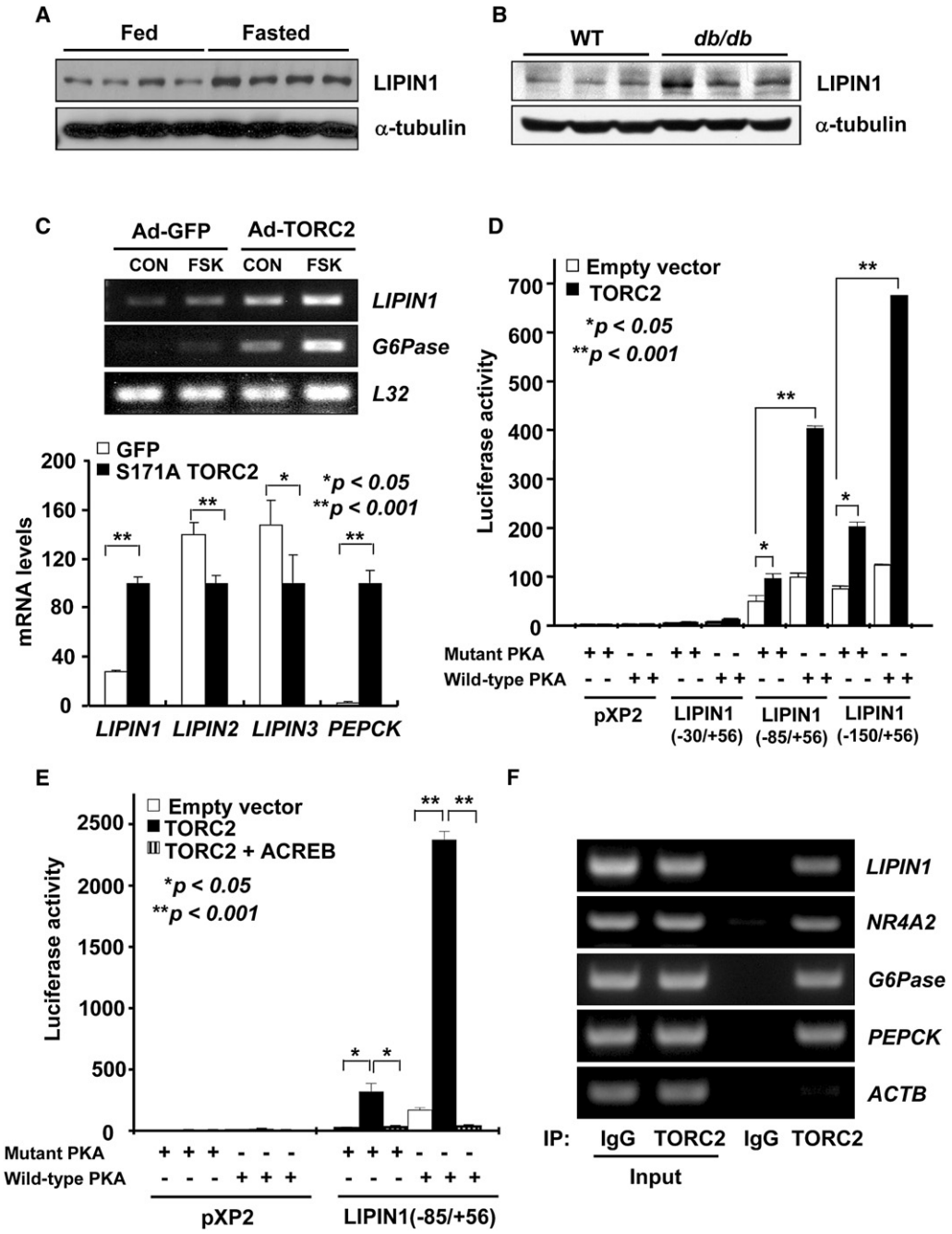

Figure 2. TORC2 Activates Transcription of Hepatic *LIPIN1*

(A) Western blot assay showing hepatic LIPIN1 expression in mice under fed or fasted conditions.

(B) Western blot assay showing hepatic LIPIN1 expression in WT or *db/db* mice.

(C) RT-PCR analysis showing effect of TORC2 pathway on mRNA levels of *LIPIN1* and *G6Pase* (top) or *LIPIN* family members and *PEPCK* (bottom) in rat primary hepatocytes. Cells were infected with adenoviruses for GFP, TORC2, or S171A TORC2 for 48 hr and then exposed to forskolin or DMSO for 2 hr (*$p < 0.05$; **$p < 0.001$; n = 3).

(D) Transient assays of HepG2 cells transfected with LIPIN1 luciferase constructs (*$p < 0.05$; **$p < 0.001$; n = 3).

(E) Transient assays of HepG2 cells transfected with LIPIN1 luciferase construct showing effects of expression vector for CREB dominant-negative polypeptide (ACREB) on *LIPIN1* transcription (*$p < 0.05$; **$p < 0.001$; n = 3).

(F) Chromatin immunoprecipitation showing the occupancy of TORC2 on *LIPIN1* and gluconeogenic promoters in mouse primary hepatocytes. Data in (C)–(E) represent mean ± SD.

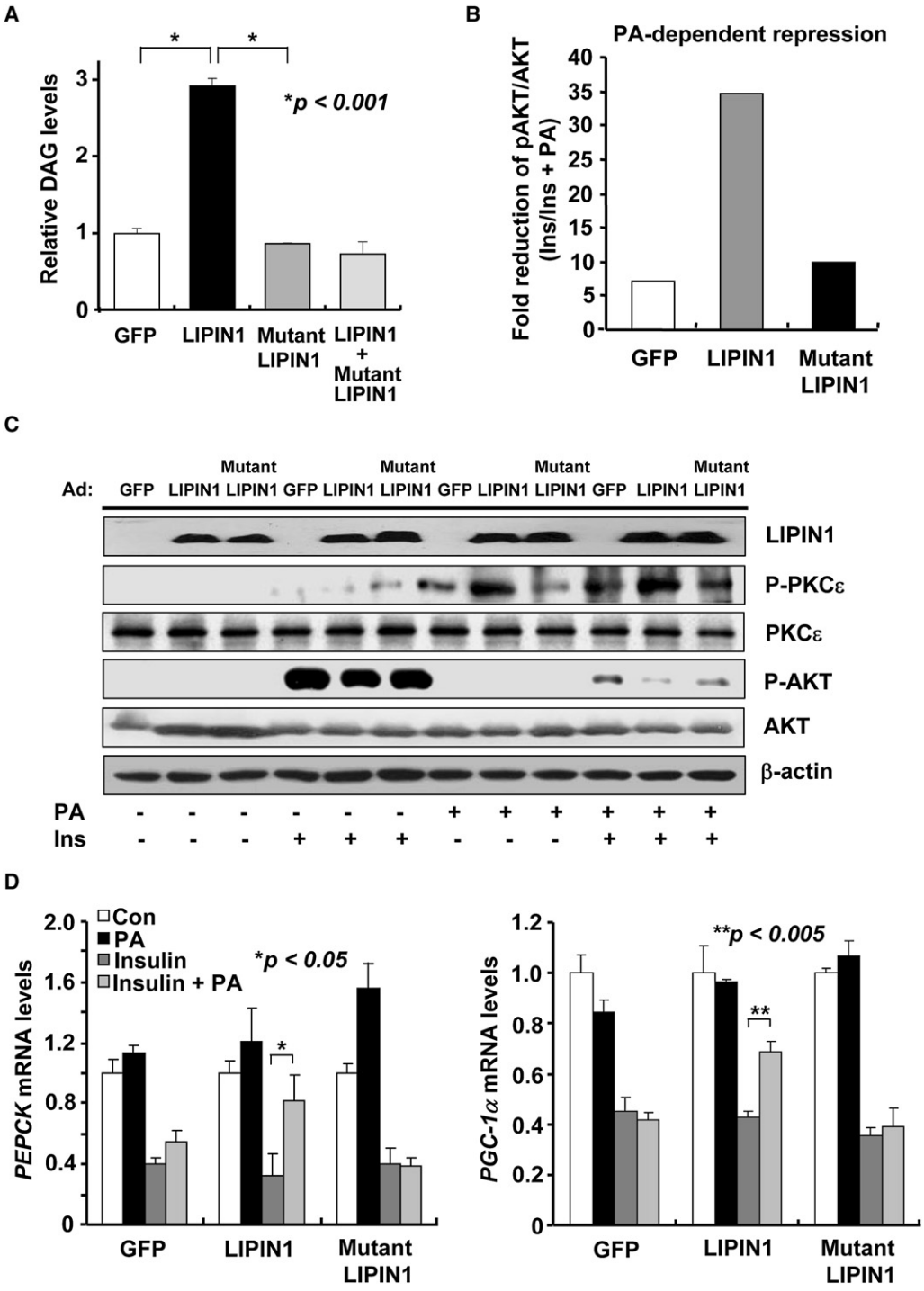

Figure 3. LIPIN1-Mediated DAG Production Is Linked to Hepatic Insulin Resistance

(A) Representative thin-layer chromatography analysis of formation of DAG in mouse primary hepatocytes infected with Ad-GFP, Ad-WT LIPIN1, or mutant Ad-LIPIN1 (D712E, D714E) (*$p < 0.001$; n = 3).

(B) Quantitation showing relative effects of PA on insulin-dependent AKT phosphorylation from cells infected with Ad-GFP, Ad-LIPIN1, or mutant Ad-LIPIN1 as in (C). The intensities of the bands were quantified by ImageJ (version 1.36×, NIH).

(C) Western blot analysis showing effects of Ad-GFP, Ad-LIPIN1, or mutant Ad-LIPIN1 on phospho-serine and total levels of AKT and PKCε. Mouse primary hepatocytes were infected with Ad-GFP, Ad-LIPIN1, or mutant Ad-LIPIN1 and then exposed to PA (50 μM) for 2 hr prior to 10 min stimulation of 100 nM insulin.

(D) Q-PCR analysis showing effect of LIPIN1 on mRNA levels of *PEPCK* (left) and *PGC-1α* (right). Cells were infected with adenoviruses for GFP, LIPIN1, or mutant LIPIN1 for 48 hr and then cultured in the absence or in the presence of 100 μM PA (2 hr) and/or 100 nM insulin (4 hr) (*$p < 0.05$; **$p < 0.005$; n = 3). Data in (A) and (D) represent mean ± SD.

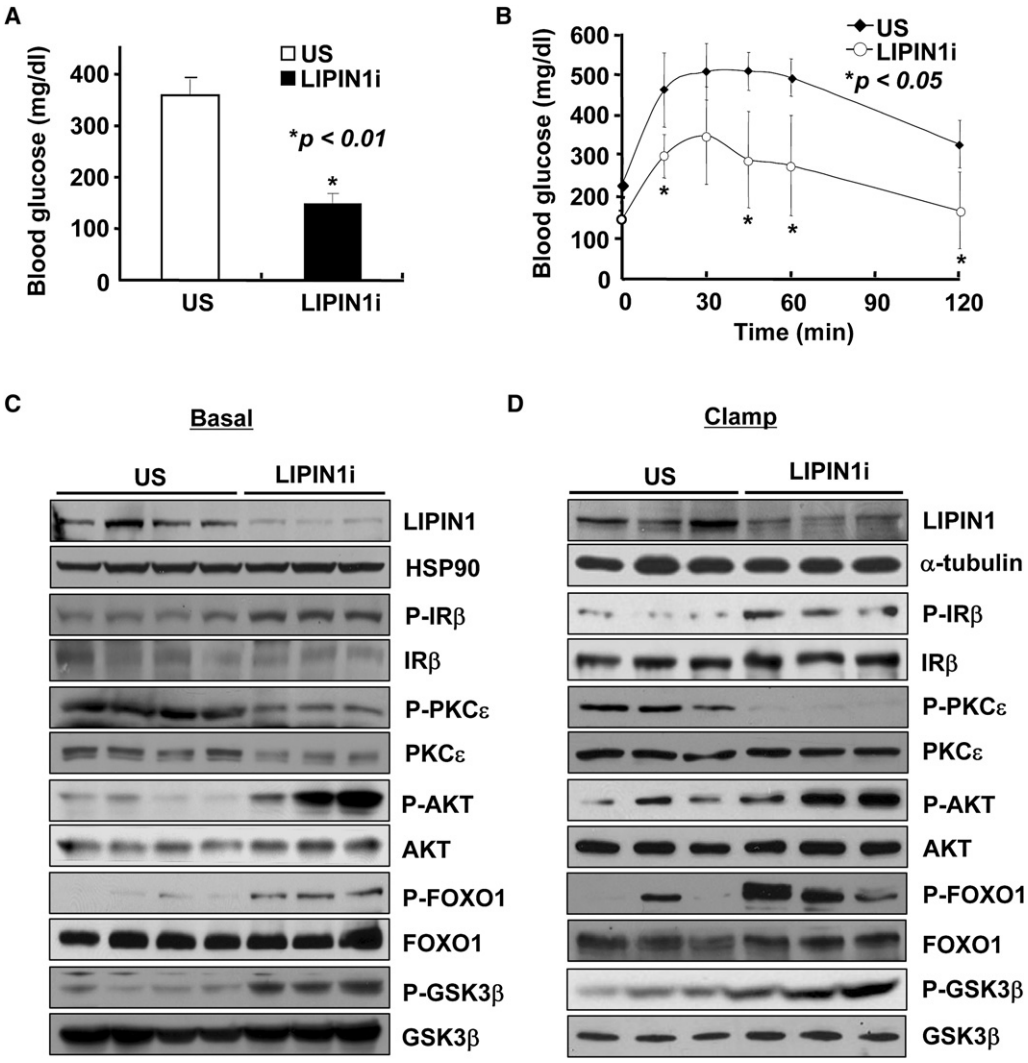

Figure 4. Knockdown of LIPIN1 Improves Hepatic Glucose Tolerance and Insulin Signaling in *db/db* Mice

(A and B) Four hour fasting glucose levels (*p < 0.01) (A) and GTT (*p < 0.05) (B) from *db/db* mice injected with either Ad-US (n = 4) or Ad-LIPIN1 RNAi (n = 3).

(C) Western blot analysis of total and phosphorylated forms of IR, PKCε, AKT, FOXO1, and GSK3β using extracts from 4 hr fasted mouse liver infected with either Ad-US or Ad-LIPIN1 RNAi virus.

(D) Western blot analysis of total and phosphorylated forms of IR, PKCε, AKT, FOXO1, and GSK3β using liver extracts generated from adenovirus-infected mice after clamp studies. (A) and (B) represent mean ± SD.

In a study conducted by Finck et al., LIPIN1 seems to also function as a coactivator for PPARα and PGC-1α to promote fatty acid beta oxidation in livers of WT C57BL/6 mice (Finck et al., 2006). In our study, we were unable to observe the reduction in expression of genes involved in the beta oxidation, such as *ACOX* or *CPT-Iα*, by LIPIN1 knockdown in *db/db* mouse liver (Figures S15 and S17). Interestingly, *PPARα* mRNA levels are significantly higher with LIPIN1 knockdown, perhaps compensating for the reduced expression of hepatic LIPIN1 in insulin-resistant condition that we tested in this study. Moreover, genes involved in the lipogenesis, such as *L-PK*, *FAS*, or *SCD-1*, were reciprocally decreased (Figure S16), suggesting that an equilibrium between fatty acid oxidation and fatty acid synthesis could be achieved even in the absence of LIPIN1. Alternatively, the presence of other LIPIN families in liver would partially compensate for the loss of LIPIN1 (Donkor et al., 2007; Reue and Zhang, 2008), although there are no significant changes in either *LIPIN2* or *LIPIN3* mRNA levels by LIPIN1 knockdown (Figures S16 and S18). The relative importance between coactivator function and PAP activity of LIPIN1 in normal or disease conditions would be an interesting subject for future studies.

While this work was under review, two reports came out regarding the role of LIPIN1 in triglyceride formation and VLDL secretion in liver. In a study conducted in cultured hepatocytes, LIPIN1 overexpression leads to increased triglyceride synthesis and secretion, whereas siRNA-mediated knockdown of LIPIN1 selectively decreased VLDL assembly and secretion among lipoproteins measured (Khalil et al., 2009). On the other hand, adenovirus-mediated overexpression of LIPIN1 in cultured *fld* mouse hepatocytes or in liver of UCP-DTA mouse, a brown-fat-deficient

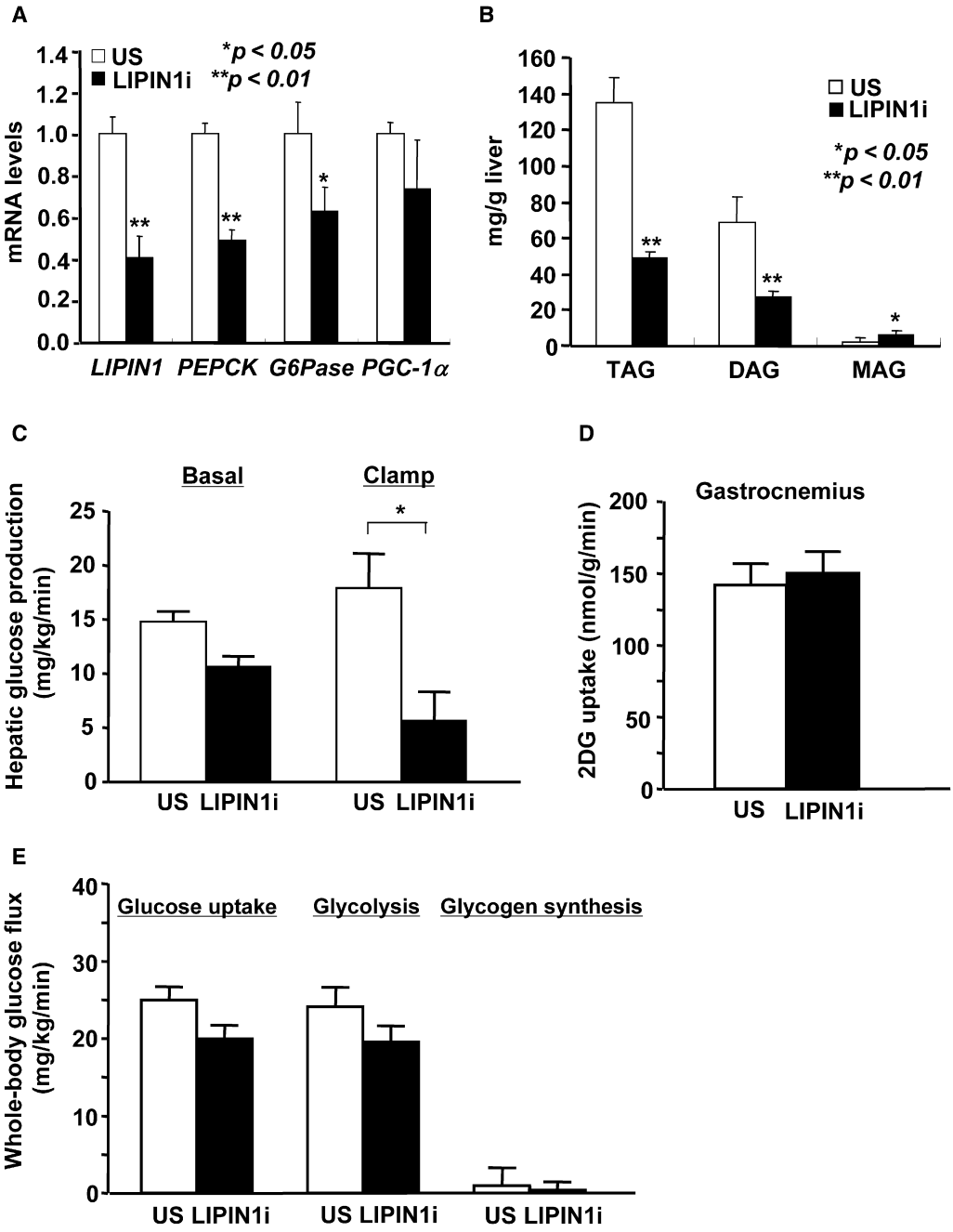

Figure 5. Knockdown of LIPIN1 Improves Hepatic Insulin Sensitivity in *db/db* Mice

(A) Q-PCR analysis showing effect of Ad-US or Ad-LIPIN1 RNAi infection on hepatic expression of gluconeogenic genes in *db/db* mice fasted for 4 hr. (*$p < 0.05$; **$p < 0.01$; $n = 3$).

(B) Tri-, di-, and mono-acylglycerols in liver of Ad-US- and Ad-LIPIN1 RNAi-injected *db/db* mice (*$p < 0.05$; **$p < 0.001$; $n = 3$).

(C–E) Peripheral and hepatic insulin sensitivity was assessed by means of hyperinsulinemic-euglycemic clamps. Shown are hepatic glucose production (C), skeletal muscle (gastrocnemius) glucose uptake (D), whole-body glucose uptake (E), and glycolysis and glycogen synthesis (*$p < 0.05$, $n = 5$). (A)–(E) represent mean ± SD.

FVB mouse model that displays hyperinsulinemia (~7500 pg/ml), significantly decreased total TAG secretion, including VLDL, showing a result somewhat inconsistent from the aforementioned study (Chen et al., 2008). To resolve differences in the proposed functions of hepatic LIPIN1, generation of liver-specific transgenic or knockout mice would be desirable to avoid secondary effects from LIPIN1 overexpression/knockout on other tissues, such as adipose tissue. These mouse models would also be useful to study the longer-term effects of hepatic LIPIN1 expression on lipid metabolism or insulin signaling in liver.

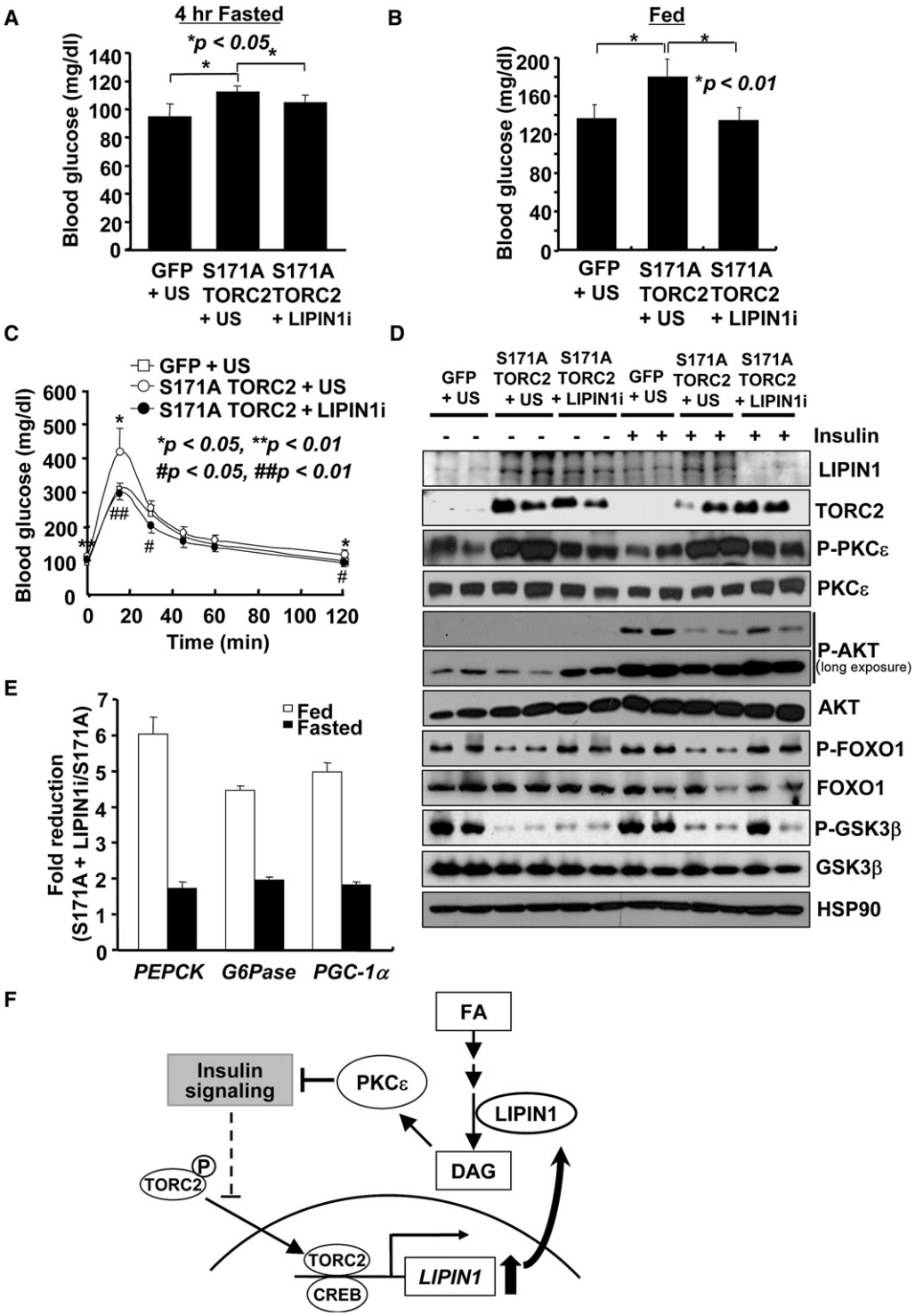

Figure 6. LIPIN1 Knockdown Improves TORC2-Induced Hepatic Glucose Intolerance in Mice

(A–B) Four hour fasting plasma glucose levels (A) and ad libitum feeding plasma glucose levels (B) of WT C57BL/6 mice infected with Ad-GFP + Ad-US (n = 5), Ad-S171A TORC2 + Ad-US (n = 4), or Ad-S171A TORC2 + Ad-LIPIN1i (n = 4) (*$p < 0.05$ for 4 hr fasting glucose and *$p < 0.01$ for ad libitum feeding glucose).

(C) GTT using mice as in (A). Statistically significant differences between GFP + US and S171A TORC2 + US (*$p < 0.05$; **$p < 0.01$) or S171A TORC2 + US and S171A TORC2 + LIPIN1i ($^{\#}p < 0.05$; $^{\#\#}p < 0.01$) were shown.

(D) Western blot analysis showing combined effects of Ad-S171A TORC2 and Ad-LIPIN1 RNAi on insulin singling pathway.

(E) Q-PCR analysis showing combined effects of Ad-S171A TORC2 and Ad-LIPIN1 RNAi on expression of gluconeogenic genes during 4 hr fasting or ad libitum feeding conditions (n = 3).

(F) A proposed model of TORC2 and LIPIN1-mediated hepatic insulin resistance. Data in (A)–(C) and (E) represent mean ± SD.

Increased accumulation of free fatty acids in peripheral tissues has long been regarded as a major predicament for the progression of insulin resistance (Chibalin et al., 2008; Holland et al., 2007; Holland and Summers, 2008; Kraegen and Cooney, 2008; Savage et al., 2007). Various metabolic intermediates, including ceramide, DAG, or their metabolites, were proposed to be major signaling molecules for activating serine/threonine kinases such as JNK, noncanonical PKC, S6K, or mTOR to target IR or IR substrates to hamper insulin signaling in the cell (Jaeschke and Davis, 2007; Nguyen et al., 2005; Samuel et al., 2004, 2007; Um et al., 2004, 2006). A recent review from Shulman's group revealed the importance of DAG as a signaling molecule to activate PKCθ in muscle or PKCε in liver to target either IR substrates or IR, respectively (Savage et al., 2007). However, results from other studies implied that increase in hepatic DAG alone may not be a direct indication for insulin resistance in liver, suggesting that the involvement of other related mechanisms, including inflammation, is further required (Choi et al., 2007b; Minehira et al., 2008; Monetti et al., 2007). In our study, decreased expression of LIPIN1 reduces cellular DAG levels that are concomitant with decreased phosphorylation of PKCε and enhanced tyrosine phosphorylation of IR in previously established insulin-resistant setting, at least supporting the hypothesis that relieving the higher hepatic DAG levels might be beneficial to improve insulin signaling and deter the progression of type 2 diabetes. Further study will be necessary to discern the relative contribution of various signaling cascades that would promote insulin-resistant phenotypes in mammals.

EXPERIMENTAL PROCEDURES

Plasmids and Recombinant Adenoviruses

LIPIN1 promoter sequences were PCR-amplified from mouse genomic DNA and inserted into the pXP2-luc vector. To generate LIPIN1 and LIPIN2 expression vectors, the coding sequences of mouse *LIPIN1* and *LIPIN2* were PCR-amplified from mouse hepatic cDNA and subcloned into pcDNA3-FLAG vector. LIPIN1 mutant (D712E, D714E) was generated using site-directed mutagenesis (Finck et al., 2006). Adenoviruses expressing GFP only, nonspecific RNAi control (US), LIPIN1, LIPIN1 RNAi, and PKCε were generated as described previously (Koo et al., 2005).

Animal Experiments

Seven-week-old male C57BL/6 or *db/db* mice were purchased from Charles River Laboratories. Recombinant adenovirus (0.5×10^9 pfu) was delivered by tail-vein injection to mice. To measure fasting blood glucose levels, animals were fasted for 16 hr or 4 hr with free access to water. For GTT, mice were fasted for 16 hr and then injected intraperitoneally with 1 g/kg (for *db/db* mice) or 2 g/kg (for C57BL/6 mice) body weight of glucose (Koo et al., 2004). Blood glucose was measured from tail-vein blood collected at the designated times.

All procedures were approved by the Sungkyunkwan University School of Medicine Institutional Animal Care and Use Committee (IACUC).

Quantitative PCR

Total RNA from either primary hepatocytes or liver tissue was extracted using RNeasy Mini Kit (QIAGEN). cDNAs generated by Superscript II enzyme (Invitrogen) were analyzed by Q-PCR using a SYBR Green PCR Kit and TP800 Thermal Cycler Dice Real Time System (TAKARA). All data were normalized to ribosomal *L32* expression.

Western Blot Analyses

Western blot analyses on 50–150 g of whole-cell extracts were performed as described (Koo et al., 2004). LIPIN1 antibody was from Novus. Antisera against IRS1, IRS2, AKT, phospho-Ser473 AKT, GSK3β, phospho-Ser9 GSK3β, FOXO1, phospho-Ser256 FOXO1, IRβ, phospho-Tyr1162/1163 IRβ, and phospho-Tyrosine were purchased from Cell Signaling. Antibodies against total PKCε and phospho-Ser729 PKCε were obtained from Upstate and Santa Cruz, respectively. Antibodies against HSP90 (Santa Cruz) and α-tubulin (Sigma) were used to assess equal loading.

Culture of Primary Hepatocytes

Primary hepatocytes were prepared from 200–300 g Sprague-Dawley rats or 8- to 10-week-old C57BL/6 mice by collagenase perfusion method as described previously (Koo et al., 2005). Cells were plated with medium 199 supplemented by 10% FBS, 10 units/ml penicillin, 10 μg/ml streptomycin, and 10 nM dexamethasone. After attachment, cells were infected with various adenoviruses, indicated in figure legends, for 16 hr. Subsequently, cells were maintained in the same media without FBS overnight and treated with 100 nM dexamethasone and 10 μM forskolin for 2 hr with or without 100 nM insulin for 16 hr.

Transfection Assays

Human hepatoma HepG2 cells were maintained with Ham's F12 medium supplemented with 10% FBS, 10 units/ml penicillin, and 10 μg/ml streptomycin. Each transfection was performed with 300 ng of luciferase construct, 50 ng of β-galactosidase plasmid, and 2.5–100 ng of expression vector for TORC2, PKA, or mutant PKA using Fugene 6 reagent, according to manufacturer's instruction.

Chromatin Immunoprecipitation Assays

Nuclear isolation, cross-linking, and chromatin immunoprecipitation assays on primary mouse hepatocyte samples were performed as described previously (Jaeschke and Davis, 2007). Precipitated DNA fragments were analyzed by PCR using primers against relevant mouse promoters.

Thin-Layer Chromatographic Analyses

Lipids from rat primary hepatocytes, which were labeled with 1 μCi/ml of [^{3}H]palmitic acid (Moravek Biochemicals, Inc.) in the serum-free medium for 18 hr, were extracted using the Bligh and Dyer method (Bligh and Dyer, 1959). DAG was separated from other phospholipids by thin-layer chromatography using a solvent system of toluene/ether/ethanol/concentrated NH_4OH (50/30/20/0.2, v/v). DAG bands corresponding to 1,2-diacyl glycerol (Avanti Polar Lipids) were identified with primulin, scraped, and counted using a scintillation counter.

Measurement of Metabolites

Blood glucose for basal conditions and during GTT was monitored from tail-vein blood using an automatic glucose monitor (OneTouch; LifeScan, Inc.). Blood triglycerides and NEFA were measured by colorimetric assay kits (Wako). Insulin was measured by Mouse Insulin ELISA Kit (U-Type; Shibayagi Corp.). Total liver lipids were extracted with chloroform-methanol (2:1, v/v) mixture according to Folch method (Folch et al., 1957). The extracts were dissolved in chloroform, and the solutions were loaded on Sep-Pak NH_2 columns (Sep-Pak Vac 6cc [500 mg] NH_2 cartridge; Waters Corp.). The fractions were separated into triacylglyceride, diacylglyceride, and monoacylglyceride (Giacometti et al., 2002; Kaluzny et al., 1985). The contents were analyzed with lipid standard (1787-1AMP, Lipid Standard, Mono-, Di-, & Triglyceride Mix; Supelco) on HPLC-ELSD system (Evaporative Light Scattering Detector [ELSD] ZAM 3000; Schambeck SFD GmbH) as described (Bravi et al., 2006).

Hyperinsulinemic-Euglycemic Clamp Study

Seven days prior to the hyperinsulinemic-euglycemic clamp studies, indwelling catheters were placed into the right internal jugular vein extending to the right atrium. After an overnight fast, [3-^{3}H]glucose (HPLC purified; PerkinElmer) was infused at a rate of 0.05 μCi/min for 2 hr to assess the basal glucose turnover. Following the basal period, hyperinsulinemic-euglycemic clamp was conducted for 140 min with a primed/continuous infusion of human insulin (210 pmol/kg prime, 30 pmol/kg/min infusion) (Novo Nordisk; Denmark). Blood samples (10 μl) were collected at 10–20 min intervals, plasma glucose was immediately analyzed during the clamps by a glucose oxidase method (GM9 Analyzer; Analox Instruments; London), and 20% dextrose

was infused at variable rates to maintain plasma glucose at basal concentrations (~6.7 mM). To estimate insulin-stimulated whole-body glucose fluxes, [3-^{3}H]glucose was infused at a rate of 0.1 μCi/min throughout the clamps, and 2-deoxy-D-[1-^{14}C]glucose (2-[^{14}C]DG; PerkinElmer) was injected as a bolus at the 85th minute of the clamp to estimate the rate of insulin-stimulated tissue glucose uptake, as previously described (Choi et al., 2007a). Blood samples (10 μl) for the measurement of plasma ^{3}H and ^{14}C activities were taken at the end of the basal period and during the last 45 min of the clamp.

Glucose Flux Calculation

For the determination of plasma [^{3}H]glucose, plasma was deproteinized with $ZnSO_4$ and $Ba(OH)_2$, dried to remove $[^3H]_2O$, resuspended in water, and counted in scintillation fluid (Ultima Gold; PerkinElmer) on a PerkinElmer scintillation counter. Rates of basal and insulin-stimulated whole-body glucose turnover were determined as the ratio of the [3-^{3}H]glucose infusion rate (disintegrations per minute [dpm]) to the specific activity of plasma glucose (dpm/mg) at the end of the basal period and during the final 30 min of the clamp experiment, respectively. Hepatic glucose production was determined by subtracting the glucose infusion rate from the total glucose appearance rate.

The plasma concentration of $[^3H]_2O$ was determined by the difference between ^{3}H counts without and with drying. Whole-body glycolysis was calculated from the rate of increase in plasma $[^3H]_2O$ concentration divided by the specific activity of plasma [^{3}H]glucose, as previously described (Youn and Buchanan, 1993). Whole-body glycogen synthesis was estimated by subtracting whole-body glycolysis from whole-body glucose uptake, assuming that glycolysis and glycogen synthesis account for the majority of insulin-stimulated glucose uptake (Rossetti and Giaccari, 1990).

Statistical Analyses

Results are shown as mean ± SD. The comparison of different groups was carried out using two-tailed unpaired Student's t test, and differences at or under to $p < 0.05$ were considered statistically significant and reported as in legends.

SUPPLEMENTAL DATA

Supplemental Data include 18 figures and can be found online at http://www.cell.com/cellmetabolism/supplemental/S1550-4131(09)00008-4.

ACKNOWLEDGMENTS

We would like to thank Sun Myung Park and Bo-Kyoung Kim for the technical assistance. This work was supported by a Research Program for New Drug Target Discovery (M10648000089-08N4800-08910) grant; a Korea Science and Engineering Foundation (KOSEF) grant (R01-2008-000-11935-0); a Korea Research Foundation (KRF) grant (2006-E00037) by the Ministry of Education, Science, and Technology; and a grant from the Marine Biotechnology Program funded by the Ministry of Land, Transport, and Maritime Affairs, Republic of Korea.

Received: July 5, 2008
Revised: November 13, 2008
Accepted: January 14, 2009
Published: March 3, 2009

REFERENCES

Bligh, E.G., and Dyer, W.J. (1959). A rapid method of total lipid extraction and purification. Can. J. Biochem. Physiol. *37*, 911–917.

Bravi, E., Perretti, G., and Montanari, L. (2006). Fatty acids by high-performance liquid chromatography and evaporative light-scattering detector. J. Chromatogr. A. *1134*, 210–214.

Carman, G.M., and Han, G.S. (2006). Roles of phosphatidate phosphatase enzymes in lipid metabolism. Trends Biochem. Sci. *31*, 694–699.

Chen, Z., Gropler, M.C., Norris, J., Lawrence, J.C., Jr., Harris, T.E., and Finck, B.N. (2008). Alterations in hepatic metabolism in fld mice reveal a role for lipin 1 in regulating VLDL-triacylglyceride secretion. Arterioscler. Thromb. Vasc. Biol. *28*, 1738–1744.

Chibalin, A.V., Leng, Y., Vieira, E., Krook, A., Bjornholm, M., Long, Y.C., Kotova, O., Zhong, Z., Sakane, F., Steiler, T., et al. (2008). Downregulation of diacylglycerol kinase delta contributes to hyperglycemia-induced insulin resistance. Cell *132*, 375–386.

Choi, C.S., Savage, D.B., Abu-Elheiga, L., Liu, Z.X., Kim, S., Kulkarni, A., Distefano, A., Hwang, Y.J., Reznick, R.M., Codella, R., et al. (2007a). Continuous fat oxidation in acetyl-CoA carboxylase 2 knockout mice increases total energy expenditure, reduces fat mass, and improves insulin sensitivity. Proc. Natl. Acad. Sci. USA *104*, 16480–16485.

Choi, C.S., Savage, D.B., Kulkarni, A., Yu, X.X., Liu, Z.X., Morino, K., Kim, S., Distefano, A., Samuel, V.T., Neschen, S., et al. (2007b). Suppression of diacylglycerol acyltransferase-2 (DGAT2), but not DGAT1, with antisense oligonucleotides reverses diet-induced hepatic steatosis and insulin resistance. J. Biol. Chem. *282*, 22678–22688.

Dentin, R., Liu, Y., Koo, S.H., Hedrick, S., Vargas, T., Heredia, J., Yates, J., 3rd, and Montminy, M. (2007). Insulin modulates gluconeogenesis by inhibition of the coactivator TORC2. Nature *449*, 366–369.

Donkor, J., Sariahmetoglu, M., Dewald, J., Brindley, D.N., and Reue, K. (2007). Three mammalian lipins act as phosphatidate phosphatases with distinct tissue expression patterns. J. Biol. Chem. *282*, 3450–3457.

Finck, B.N., Gropler, M.C., Chen, Z., Leone, T.C., Croce, M.A., Harris, T.E., Lawrence, J.C., Jr., and Kelly, D.P. (2006). Lipin 1 is an inducible amplifier of the hepatic PGC-1alpha/PPARalpha regulatory pathway. Cell Metab. *4*, 199–210.

Folch, J., Lees, M., and Sloane Stanley, G.H. (1957). A simple method for the isolation and purification of total lipides from animal tissues. J. Biol. Chem. *226*, 497–509.

Giacometti, J., Milosevic, A., and Milin, C. (2002). Gas chromatographic determination of fatty acids contained in different lipid classes after their separation by solid-phase extraction. J. Chromatogr. A. *976*, 47–54.

Han, G.S., Wu, W.I., and Carman, G.M. (2006). The Saccharomyces cerevisiae Lipin homolog is a Mg2+-dependent phosphatidate phosphatase enzyme. J. Biol. Chem. *281*, 9210–9218.

Han, G.S., Siniossoglou, S., and Carman, G.M. (2007). The cellular functions of the yeast lipin homolog PAH1p are dependent on its phosphatidate phosphatase activity. J. Biol. Chem. *282*, 37026–37035.

Holland, W.L., and Summers, S.A. (2008). Sphingolipids, insulin resistance, and metabolic disease: new insights from in vivo manipulation of sphingolipid metabolism. Endocr. Rev. *29*, 381–402.

Holland, W.L., Knotts, T.A., Chavez, J.A., Wang, L.P., Hoehn, K.L., and Summers, S.A. (2007). Lipid mediators of insulin resistance. Nutr. Rev. *65*, S39–S46.

Jaeschke, A., and Davis, R.J. (2007). Metabolic stress signaling mediated by mixed-lineage kinases. Mol. Cell *27*, 498–508.

Kaluzny, M.A., Duncan, L.A., Merritt, M.V., and Epps, D.E. (1985). Rapid separation of lipid classes in high yield and purity using bonded phase columns. J. Lipid Res. *26*, 135–140.

Khalil, M.B., Sundaram, M., Zhang, H.Y., Links, P.H., Raven, J.F., Manmontri, B., Sariahmetoglu, M., Tran, K., Reue, K., Brindley, D.N., and Yao, Z. (2009). The level and compartmentalization of phosphatidate phosphatase-1 (lipin-1) control the assembly and secretion of hepatic VLDL. J. Lipid Res. *50*, 47–58.

Koo, S.H., Satoh, H., Herzig, S., Lee, C.H., Hedrick, S., Kulkarni, R., Evans, R.M., Olefsky, J., and Montminy, M. (2004). PGC-1 promotes insulin resistance in liver through PPAR-alpha-dependent induction of TRB-3. Nat. Med. *10*, 530–534.

Koo, S.H., Flechner, L., Qi, L., Zhang, X., Screaton, R.A., Jeffries, S., Hedrick, S., Xu, W., Boussouar, F., Brindle, P., et al. (2005). The CREB coactivator TORC2 is a key regulator of fasting glucose metabolism. Nature *437*, 1109–1111.

Kraegen, E.W., and Cooney, G.J. (2008). Free fatty acids and skeletal muscle insulin resistance. Curr. Opin. Lipidol. *19*, 235–241.

Minehira, K., Young, S.G., Villanueva, C.J., Yetukuri, L., Oresic, M., Hellerstein, M.K., Farese, R.V., Jr., Horton, J.D., Preitner, F., Thorens, B., and Tappy, L. (2008). Blocking VLDL secretion causes hepatic steatosis but does not affect peripheral lipid stores or insulin sensitivity in mice. J. Lipid Res. *49*, 2038–2044.

Monetti, M., Levin, M.C., Watt, M.J., Sajan, M.P., Marmor, S., Hubbard, B.K., Stevens, R.D., Bain, J.R., Newgard, C.B., Farese, R.V., Sr., et al. (2007). Dissociation of hepatic steatosis and insulin resistance in mice overexpressing DGAT in the liver. Cell Metab. *6*, 69–78.

Nguyen, M.T., Satoh, H., Favelyukis, S., Babendure, J.L., Imamura, T., Sbodio, J.I., Zalevsky, J., Dahiyat, B.I., Chi, N.W., and Olefsky, J.M. (2005). JNK and tumor necrosis factor-alpha mediate free fatty acid-induced insulin resistance in 3T3-L1 adipocytes. J. Biol. Chem. *280*, 35361–35371.

Peterfy, M., Phan, J., Xu, P., and Reue, K. (2001). Lipodystrophy in the fld mouse results from mutation of a new gene encoding a nuclear protein, lipin. Nat. Genet. *27*, 121–124.

Peterfy, M., Phan, J., and Reue, K. (2005). Alternatively spliced lipin isoforms exhibit distinct expression pattern, subcellular localization, and role in adipogenesis. J. Biol. Chem. *280*, 32883–32889.

Phan, J., and Reue, K. (2005). Lipin, a lipodystrophy and obesity gene. Cell Metab. *1*, 73–83.

Phan, J., Peterfy, M., and Reue, K. (2004). Lipin expression preceding peroxisome proliferator-activated receptor-gamma is critical for adipogenesis in vivo and in vitro. J. Biol. Chem. *279*, 29558–29564.

Reue, K., and Dwyer, J.R. (2008). Lipin proteins and metabolic homeostasis. J. Lipid Res., in press. Published online October 21, 2008. 10.1194/jlr.R800052-JLR200.

Reue, K., and Zhang, P. (2008). The lipin protein family: dual roles in lipid biosynthesis and gene expression. FEBS Lett. *582*, 90–96.

Rossetti, L., and Giaccari, A. (1990). Relative contribution of glycogen synthesis and glycolysis to insulin-mediated glucose uptake. A dose-response euglycemic clamp study in normal and diabetic rats. J. Clin. Invest. *85*, 1785–1792.

Samuel, V.T., Liu, Z.X., Qu, X., Elder, B.D., Bilz, S., Befroy, D., Romanelli, A.J., and Shulman, G.I. (2004). Mechanism of hepatic insulin resistance in nonalcoholic fatty liver disease. J. Biol. Chem. *279*, 32345–32353.

Samuel, V.T., Liu, Z.X., Wang, A., Beddow, S.A., Geisler, J.G., Kahn, M., Zhang, X.M., Monia, B.P., Bhanot, S., and Shulman, G.I. (2007). Inhibition of protein kinase Cepsilon prevents hepatic insulin resistance in nonalcoholic fatty liver disease. J. Clin. Invest. *117*, 739–745.

Savage, D.B., Petersen, K.F., and Shulman, G.I. (2007). Disordered lipid metabolism and the pathogenesis of insulin resistance. Physiol. Rev. *87*, 507–520.

Screaton, R.A., Conkright, M.D., Katoh, Y., Best, J.L., Canettieri, G., Jeffries, S., Guzman, E., Niessen, S., Yates, J.R., 3rd, Takemori, H., et al. (2004). The CREB coactivator TORC2 functions as a calcium- and cAMP-sensitive coincidence detector. Cell *119*, 61–74.

Shaw, R.J., Lamia, K.A., Vasquez, D., Koo, S.H., Bardeesy, N., Depinho, R.A., Montminy, M., and Cantley, L.C. (2005). The kinase LKB1 mediates glucose homeostasis in liver and therapeutic effects of metformin. Science *310*, 1642–1646.

Um, S.H., Frigerio, F., Watanabe, M., Picard, F., Joaquin, M., Sticker, M., Fumagalli, S., Allegrini, P.R., Kozma, S.C., Auwerx, J., and Thomas, G. (2004). Absence of S6K1 protects against age- and diet-induced obesity while enhancing insulin sensitivity. Nature *431*, 200–205.

Um, S.H., D'Alessio, D., and Thomas, G. (2006). Nutrient overload, insulin resistance, and ribosomal protein S6 kinase 1, S6K1. Cell Metab. *3*, 393–402.

Verheijen, M.H., Chrast, R., Burrola, P., and Lemke, G. (2003). Local regulation of fat metabolism in peripheral nerves. Genes Dev. *17*, 2450–2464.

Youn, J.H., and Buchanan, T.A. (1993). Fasting does not impair insulin-stimulated glucose uptake but alters intracellular glucose metabolism in conscious rats. Diabetes *42*, 757–763.